Catalysis Today 176 (2011) 229–233

Contents lists available at ScienceDirect

Catalysis Today

journal homepage: www.elsevier.com/locate/cattod

Influence of the state of iron on CO oxidation on FeSiBEA zeolite catalysts

Izabela Hnat[a], Ireneusz Kocemba[a], Jacek Rynkowski[a,*], Thomas Onfroy[b], Stanislaw Dzwigaj[b,**]

[a] Institute of General and Ecological Chemistry, Technical University of Lodz, Zeromskiego 116, 90-924 Lodz, Poland
[b] Laboratoire de Réactivité de Surface, UMR 7197-CNRS, Université Pierre et Marie Curie, 4 place Jussieu, 75252 Paris, France

ARTICLE INFO

Article history:
Received 10 October 2010
Received in revised form
19 December 2010
Accepted 22 December 2010
Available online 5 February 2011

Keywords:
BEA
Zeolite
Iron
FTIR
TPR
DR UV–vis
Pyridine
CO
Oxidation

ABSTRACT

The influence of the state of iron on the catalytic properties of Fe_xSiBEA zeolite in the oxidation of CO was investigated. Various Fe_xSiBEA zeolites (x = 0.6, 1.0, 4.0 and 10 wt%) were prepared by a two-step post synthesis method. The presence of Fe(III) in tetrahedral coordination for low Fe content and tetrahedral and octahedral coordination for high Fe content is evidenced by diffuse reflectance UV–Vis and TPR. FTIR investigations of pyridine adsorption show that Brønsted and Lewis acidic sites are formed upon incorporation of iron in SiBEA zeolite. The amount of both acidic sites increases with Fe content. The catalytic activity of Fe_xSiBEA in the oxidation of CO strongly depends on the state of iron in BEA structure. $Fe_{0.6}$SiBEA and $Fe_{1.0}$SiBEA containing mainly framework tetrahedral Fe(III) ions are more active than Fe_{10}SiBEA containing mainly extra-framework FeO_x oligomers. The most active catalyst is Red-$Fe_{1.0}$SiBEA obtained after reduction of $Fe_{1.0}$SiBEA at 760 °C in flowing H_2. It shows almost 100% CO conversion at room temperature.

1. Introduction

The unique physicochemical properties of zeolites have made them the most interesting class of materials for various catalytic applications [1]. Zeolites containing iron ions are active in great numbers of reactions, including decomposition of nitrogen oxides [2,3], selective catalytic reduction with hydrocarbons [4,5] or CO oxidation [6]. Introduction of iron ions into the zeolite structure leads to obtain a material with very good catalytic properties. Recently [7–9], it was shown that catalytic activity strongly depends on the nature and state of iron introduced into the zeolite structure. The investigations performed by Szegedi et al. [6] show that the Fe ions introduced into BEA zeolite structure may seem to be active sites of CO oxidation. However, a relation between iron state and catalytic properties of Fe-containing BEA zeolite was not well established.

In the present work, we report the influence of the state of iron on the catalytic properties of Fe_xSiBEA zeolite in the oxidation of CO. The state of iron species was characterised using different techniques such as XRD, TPR, FTIR and DR UV–vis.

2. Experimental

2.1. Catalyst preparation

Fe_xSiBEA catalysts (x = 0.6, 1.0, 4.0 and 10 wt% Fe) were prepared by the two-step post synthesis method reported earlier [10,11]. To obtain samples with different Fe contents, 2 g of siliceous BEA zeolite (Si/Al = 1300), obtained by treatment of a tetraethyl ammonium (TEA) BEA zeolite (Si/Al = 12.5) in a 13 mol L^{-1} HNO_3 solution (4 h, 80 °C) was stirred for 24 h at 25 °C in aqueous solutions containing from 0.7×10^{-3} to 3.9×10^{-2} mol L^{-1} of $Fe(NO_3)_3 \cdot 9H_2O$. Then, the suspensions were stirred for 2 h in air at 80 °C until evaporation of water and obtained dry solids. The solids with 0.6, 1.0, 4.0 and 10 wt% Fe are labelled $Fe_{0.6}$SiBEA, $Fe_{1.0}$SiBEA, $Fe_{4.0}$SiBEA and Fe_{10}SiBEA, respectively. The Red-$Fe_{1.0}$SiBEA was obtained by the reduction of $Fe_{1.0}$SiBEA (0.15 g) with hydrogen stream (flow 40 ml min^{-1}) for 15 min and a linear ramp rate 15 °C min^{-1}.

2.2. Catalyst characterisation

Chemical analysis of the catalysts was performed with inductively coupled plasma atom emission spectroscopy at the CNRS Centre of Chemical Analysis (Vernaison, France).

Powder X-ray diffractograms (XRD) were recorded on a BRUKER D8 Advance diffractometer using the CuK_a radiation (λ = 154.05 pm).

* Corresponding author.
** Corresponding author. Tel.: +33 1 44 27 52 91; fax: +33 1 44 27 60 33.
E-mail addresses: jacryn@p.lodz.pl (J. Rynkowski), stanislaw.dzwigaj@upmc.fr (S. Dzwigaj).

0920-5861/$ – see front matter © 2011 Elsevier B.V. All rights reserved.
doi:10.1016/j.cattod.2010.12.052

The specific surface area and pore volume of samples were determined from N_2 adsorption data obtained at −195 °C using an ASAP 2010 Micromeritics instrument. Prior to the analysis, the samples were outgassed first at room temperature and then at 350 °C until a stable static vacuum of 0.25 Pa was reached. The specific surface area was obtained using the Brunauer–Emmett–Teller (BET) equation. The microporous pore volume was determined from the amount of N_2 adsorbed up to $P/P_0 = 0.24$.

FTIR spectra were recorded on Bruker Vector 22 spectrometer equipped with DTGS detector with resolution 2.0 cm^{-1} and number of scans 128. Samples were pressed at ~0.2 tons cm^{-2} into thin wafers of ca. 10 mg cm^{-2} and placed inside the IR cell. The wafers were calcined at 450 °C for 3 h in O_2 (100 Torr) and then outgassed at 300 °C (10^{-3} Pa) for 1 h. These wafers were contacted at room temperature with gaseous pyridine (1 Torr) via a separate cell contacting liquid pyridine. After saturation with pyridine, the samples were outgassed at 150 °C (10^{-3} Pa). FTIR spectra were recorded at room temperature in the range 4000–400 cm^{-1}.

Hydrogen temperature-programmed reduction (TPR) was carried out in a flow of 5% of H_2 in Ar (25 ml/min). The sample was placed in a quartz microreactor and the quantitative consumption of H_2 from 25 to 960 °C (7.5 °C/min) was monitored by a TCD detector.

DR UV–Vis spectra were recorded at ambient atmosphere on a Cary 5000 Varian spectrometer equipped with a double integrator with polytetrafluoroethylene as reference.

2.3. Catalyst activity measurements

Temperature-programmed surface reaction (TPSR) method [12,13] was used to measure catalytic activity in the temperature range 25–760 °C using Peak 4 apparatus, constructed in Institute of General and Ecological Chemistry [13]. The mass of the sample of 0.15 g, the stream of the reacting gases CO/air (0.20 vol.% CO and 99.80 vol.% air) or (0.35 vol.% CO and 99.65 vol.% air) and a linear ramp rate of 15 °C/min were used. The concentration of CO_2 was constantly measured by the CO_2 infrared gas analyser (Fuji Electric System Co., type ZRJ-4). Prior to CO oxidation, the SiBEA and Fe_xSiBEA were treated by calcination at 500 °C in air for 3 h and then calcined in O_2 stream at a temperature range 200–760 °C for 5 min.

3. Results and discussion

3.1. Crystalline structure and acidity of Fe_xSiBEA

3.1.1. X-ray diffraction and BET

The XRD patterns of SiBEA and Fe_xSiBEA are similar (not shown) and characteristic for BEA zeolite. The absence of diffraction lines due to extra-framework compounds in Fe_xSiBEA indicates a good dispersion of iron. The XRD patterns also show that the incorporation of iron into SiBEA does not affect the zeolite crystallinity.

The nitrogen adsorption/desorption isotherm of SiBEA and Fe_xSiBEA is of type I (Fig. 1). Isotherm analysis shows that all materials have similar BET surface area (~700 m^2 g^{-1}) and that the synthesis of Fe_xSiBEA does not lead to formation of mesopores. It can then be concluded that, in agreement with XRD results, the iron incorporation preserve the crystallinity of SiBEA zeolite.

3.1.2. FT-IR

As shown earlier [10,11], the FT-IR spectrum of TEABEA zeolite calcined at 550 °C for 15 h exhibits five IR bands due to the OH stretching modes of AlO–H groups at 3781 and 3665 cm^{-1}, Si–O(H)–Al groups at 3609 cm^{-1}, isolated SiO–H groups at 3740 cm^{-1} and H-bonded SiO–H groups at 3520 cm^{-1}.

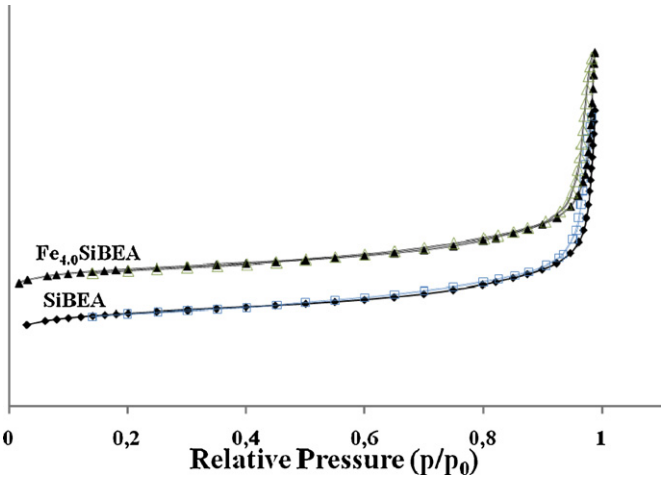

Fig. 1. Adsorption isotherms of nitrogen at −196 °C of SiBEA and $Fe_{4.0}$SiBEA. The calcined samples are evacuated at room temperature and then at 350 °C until a residual pressure below 0.2 Pa. Full symbols: adsorption; empty symbols: desorption. For convenience, the dataset for the SiBEA sample is shifted upwards along the *Y*-axis.

The treatment of (TEA)BEA zeolite by aqueous HNO_3 solution leads to the elimination of framework Al atoms, as evidenced by the disappearance of bands at 3781 and 3665 (AlO–H groups) and 3609 cm^{-1} (Si–O(H)–Al groups), in line with earlier reports [10,11]. The appearance of narrow bands at 3735 and 3714 cm^{-1} related to isolated internal and terminal silanol groups and of a broad band at 3540 cm^{-1} due to H-bonded SiOH groups in SiBEA reveals the presence of vacant T-atom sites associated with silanol groups.

The impregnation of SiBEA with aqueous $Fe(NO_3)_3$ solution reduces the intensity of the latter bands, particularly that at 3540 cm^{-1} (Fig. 2), suggesting that iron precursor react with silanol groups. Simultaneously, a FTIR band at about 3640 cm^{-1} appear corresponding to the incorporation of iron ions into vacant T-atom sites and assigned to bridging $\equiv Fe^{3+}$–O(H)–Si$\equiv$ hydroxyl, in line with earlier report [14]. The intensity of this band increases with iron content.

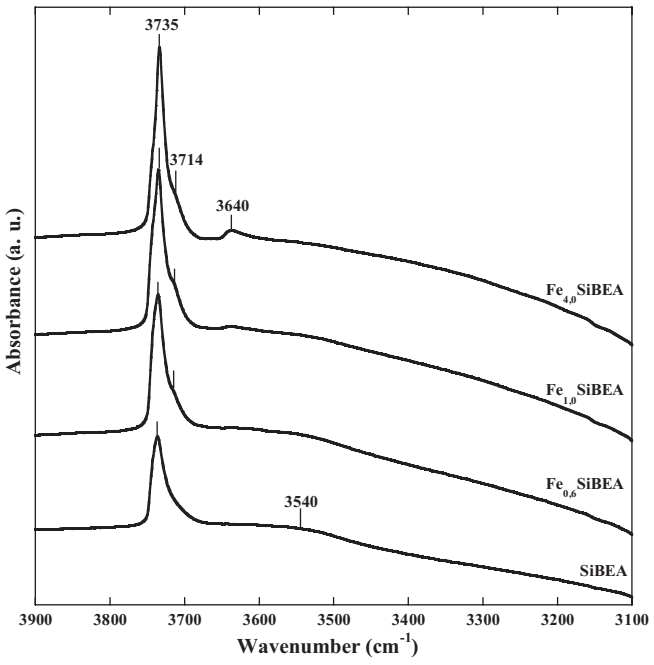

Fig. 2. FTIR spectra recorded at room temperature of SiBEA, $Fe_{0.6}$SiBEA, $Fe_{1.0}$SiBEA, and $Fe_{4.0}$SiBEA in the vibrational range of OH groups.

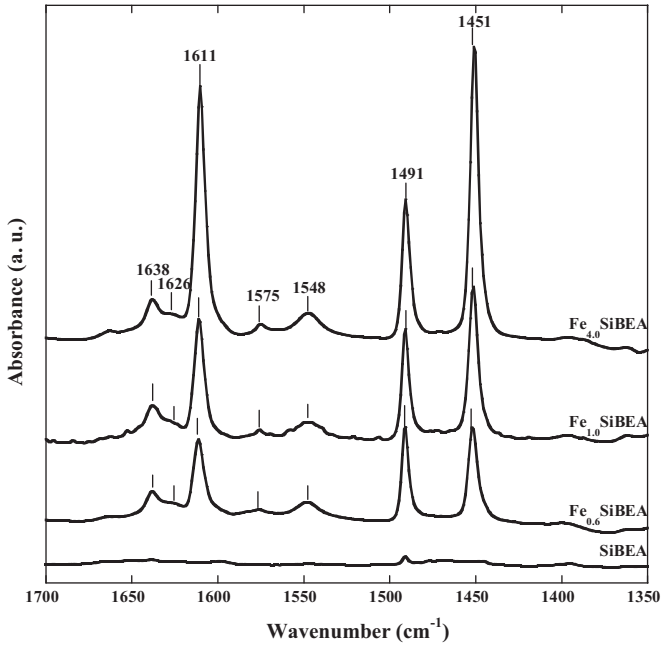

Fig. 3. FTIR spectra recorded at room temperature after adsorption of pyridine at room temperature and then outgassing at 150 °C for 0.5 h of SiBEA, $Fe_{0.6}$SiBEA, $Fe_{1.0}$SiBEA and $Fe_{4.0}$SiBEA.

The type and number of acidic sites in SiBEA and Fe_xSiBEA were probed by using pyridine. The FTIR spectra of these samples, calcined at 450 °C for 3 h and outgassed at 300 °C (10^{-3} Pa), after adsorption of pyridine at room temperature and then outgassed at 150 °C (10^{-3} Pa) for 1 h are given in Fig. 3. For SiBEA, the small bands observed at 1446, 1596 and 1608 cm^{-1} correspond to pyridine interacting with weak Lewis acidic sites and/or to pyridine physisorbed, in line with earlier data for BEA system [11]. Two bands typical of pyridinium cations are not observed at 1548 and 1638 cm^{-1} for SiBEA, indicating the absence of Brønsted acidic sites.

The introduction of iron in SiBEA leading to Fe_xSiBEA generates bands at 1548 and 1638 cm^{-1} indicating the creation of strong Brønsted acidic sites. The bands at 1451 and 1626 cm^{-1} correspond to pyridine interacting with strong Lewis acidic sites and these at 1575 and 1611 cm^{-1} (Fig. 3) to pyridine interacting with weak Lewis acidic sites (hydroxyls and/or pyridine physisorbed), in line with earlier data for BEA system [10]. The band at 1491 cm^{-1} corresponds simultaneously to both Brønsted and Lewis acidic sites.

The Brønsted acidic sites evidenced in Fe_xSiBEA are related to acidic OH groups in $\equiv Fe^{3+}–O(H)–Si\equiv$ as deduced from their disappearance upon adsorption of pyridine (results not shown).

3.2. Reducibility of the framework and extra-framework Fe(III)

The reducibility of the framework and extra-framework Fe(III) present in $Fe_{1.0}$SiBEA and Fe_{10}SiBEA has been investigated by temperature programmed reduction (TPR) under flowing hydrogen (5% H_2 in Ar). Only one peak appears for $Fe_{1.0}$SiBEA at 420 °C and three main peaks at 404, 495 and 774 °C for Fe_{10}SiBEA (Fig. 4). The peak observed at 420 °C for $Fe_{1.0}$SiBEA could be attributed to reduction of framework tetrahedral iron species from Fe(III) to Fe(II) oxidation state, in line with earlier report on Fe-imp/mordenite and Fe-BEA zeolite [15,16]. In contrast three main peaks observed for Fe_{10}SiBEA at 404, 495 and 774 °C could be attributed to reduction of framework tetrahedral Fe(III) to Fe(II), extra-framework Fe_2O_3 to Fe_3O_4 and Fe_3O_4 to metallic iron, respectively, in line with earlier work on FeHY, FeBEA and Fe/ZSM-5 [15–18].

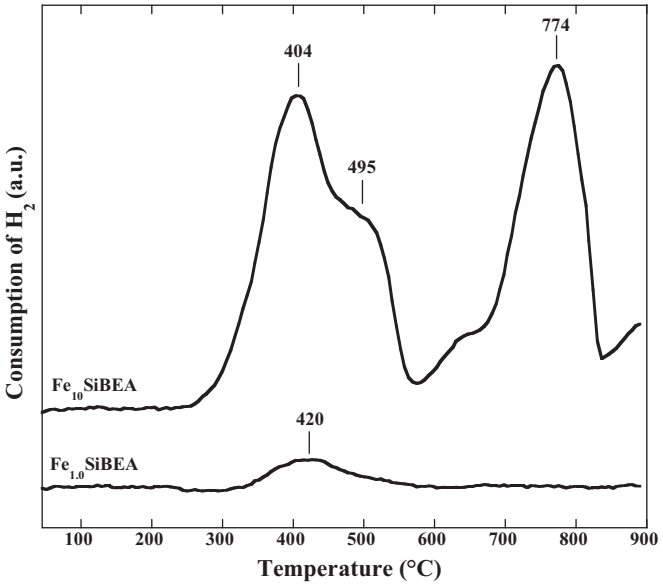

Fig. 4. TPR profiles of $Fe_{1.0}$SiBEA and Fe_{10}SiBEA after their calcination in air for 3 h at 500 °C.

The absence of a peak corresponding to reduction of Fe(II) to Fe(0) for $Fe_{1.0}$SiBEA suggests that the reducibility of framework Fe(II) to Fe(0) is much lower than that of extra-framework Fe(II) appears for Fe_{10}SiBEA (peak at 774 °C). It is probable that reduction of framework Fe(II) to Fe(0) claims much higher temperature than that used in this TPR measurements.

3.3. State of the iron in the Fe_xSiBEA zeolites

3.3.1. Diffuse reflectance UV–vis spectroscopy

Fig. 5 shows the DR UV–Vis spectra of Fe_xSiBEA samples. Samples $Fe_{0.6}$SiBEA, $Fe_{1.0}$SiBEA, and $Fe_{4.0}$SiBEA exhibit bands at 273, 264 and 270 nm, respectively, assigned to oxygen-to-metal charge transfer (CT) transitions involving tetrahedral Fe(III) ions, in line with earlier results [19,20].

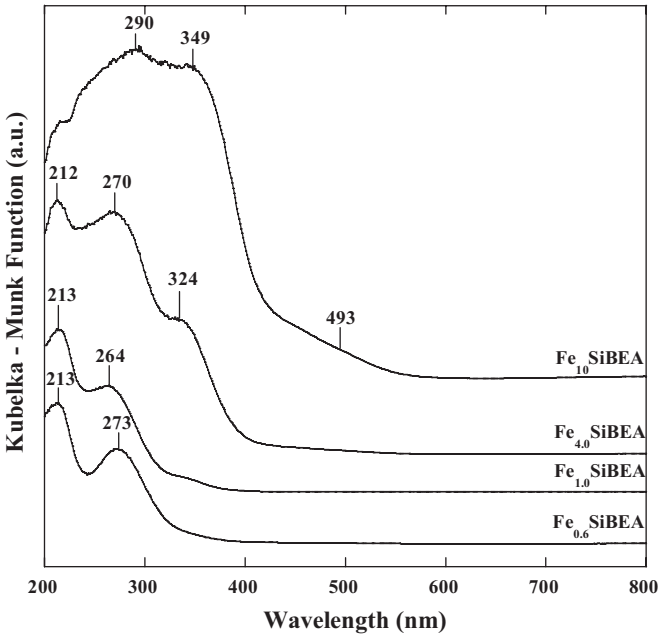

Fig. 5. DR UV–vis spectra recorded at room temperature and ambient atmosphere of $Fe_{0.6}$SiBEA, $Fe_{1.0}$SiBEA, $Fe_{4.0}$SiBEA and Fe_{10}SiBEA.

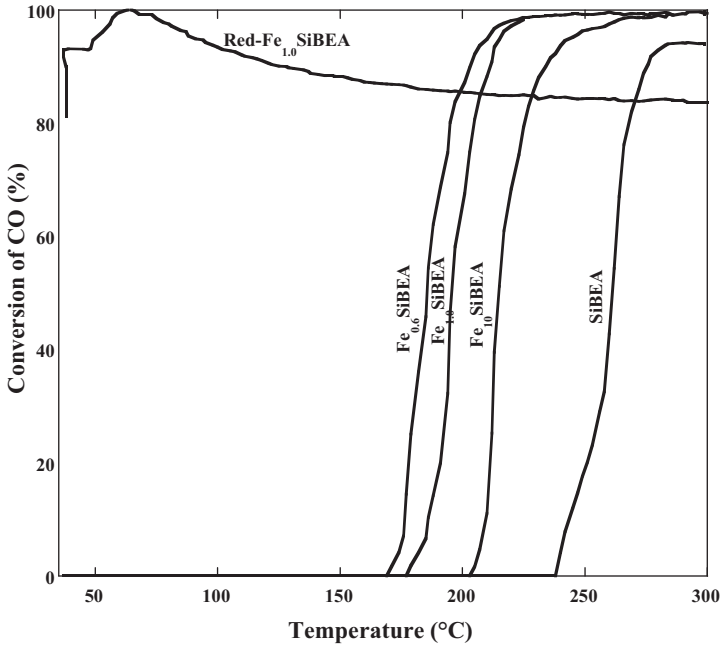

Fig. 6. Temperature-dependence of CO conversion in CO oxidation by O_2 on the SiBEA, $Fe_{0.6}$SiBEA, $Fe_{1.0}$SiBEA, Red-$Fe_{1.0}$SiBEA and Fe_{10}SiBEA.

DR UV–vis bands at 324 and 349 nm observed respectively for $Fe_{4.0}$SiBEA and Fe_{10}SiBEA can be attributed to oxygen-to-metal CT transitions involving Fe(III) in octahedral environment of oxygen atoms as reported earlier [21]. Moreover, for these samples a broad band near 400–550 nm is observed which can be assigned to the presence of extra-framework FeO_x oligomers and/or iron oxide, in line with earlier studies [14,21,22].

These DR UV–vis results show that the catalysts with low Fe content ($Fe_{0.6}$SiBEA and $Fe_{1.0}$SiBEA) contain mainly isolated tetrahedral Fe(III) species in framework of zeolite. In contrast, the catalysts with high Fe content ($Fe_{4.0}$SiBEA and Fe_{10}SiBEA) contain mainly FeO_x oligomers and/or iron oxide in extra-framework position. We can expect that this fact can have effect on their different catalytic activities in oxidation of CO.

3.4. Oxidation of CO

Fig. 6 shows the temperature-dependence of CO conversion in CO oxidation by O_2 on the SiBEA and Fe_xSiBEA catalysts. Catalysts with low Fe content show higher activity than samples with high Fe content. This suggests that catalytic activity in CO oxidation depend on the state of iron present in Fe_xSiBEA catalysts. $Fe_{0.6}$SiBEA catalyst start to be active already at 169 °C, while Fe_{10}SiBEA only at 203 °C. SiBEA use as a reference starts to be active in higher temperature (238 °C). It suggests that Fe species introduced into SiBEA are active site of CO oxidation. It seems that the highest conversion of $Fe_{0.6}$SiBEA in CO oxidation is related to the presence of isolated tetrahedral Fe(III) species in its zeolite framework. In contrast, the smaller catalytic activity of Fe_{10}SiBEA can be related to the presence in this catalyst mainly extra-framework FeO_x oligomers and/or iron oxide, as evidenced by DR UV–vis (Fig. 5). The Cu-ZSM-5 catalyst with extra-framework Cu species showed similar properties, as reported earlier by Oleksenko et al. [23].

To check the effect of the reduction of $Fe_{1.0}$SiBEA, containing only tetrahedral Fe(III) species, on its catalytic activity in CO oxidation, this sample was treated in flowing H_2. Because in a TPR pattern appears only one peak at 420 °C (Fig. 4) corresponding to reduction of tetrahedral Fe(III) to Fe(II), the treatment of the $Fe_{1.0}$SiBEA with H_2 before catalytic test was performed at 760 °C to reduce all tetrahedral Fe(III) species.

The most striking feature presented in Fig. 6 is that catalyst after reduction (Red-$Fe_{1.0}$SiBEA) is the most active catalyst those among studied in this work, showing almost 100% CO conversion at room temperature. It suggests that reduction of framework Fe(III) species leads to the formation of very active site of CO oxidation. This catalyst is more active than Cu/BEA or Cu/Pt/BEA catalyst known as efficient catalyst of CO oxidation [24]. Moreover, catalytic activity of Red-$Fe_{1.0}$SiBEA is comparable to the activity of bimetallic catalysts, in line with earlier works [7,25].

4. Conclusions

The study presented in this work shows that two-step postsynthesis method used for the preparation of Fe_xSiBEA catalysts allows, for low Fe content (<1.0 wt%), to incorporate iron zeolite framework mainly as isolated tetrahedral Fe(III) species. For higher iron content, besides the isolated tetrahedral Fe(III) ions, the octahedral Fe(III) species are formed in extra-framework positions.

The reducibility of framework tetrahedral and extra-framework octahedral Fe(III) to Fe(II) is relatively high (peaks of reduction appear at 404, 420 and 495 °C, respectively), in contrast the reducibility of Fe(II) into Fe(0) is much lower for framework Fe(II) (peak does not appear in the TPR pattern) than for extra-framework Fe(II) (peak appears at 774 °C).

Well dispersed tetrahedral Fe(III) present in framework of zeolite is more active in CO oxidation than oligomers and/or iron oxide present in extra-framework positions. It seems that the catalyst with the lowest Fe content ($Fe_{0.6}$SiBEA) shows the highest activity because it contains only tetrahedral iron species, which are responsible for formation of Brønsted and Lewis acidic sites. These sites are very good candidates as adsorption sites of CO.

The most striking feature presented results is that catalyst after reduction (Red-$Fe_{1.0}$SiBEA) is the most active catalyst from among studied in this work (it shows almost 100% conversion in room temperature).

Further studies are undertaken to better understand the CO oxidation process on Fe_xSiBEA system reduced in different conditions (by H_2 and/or CO) by in situ DRIFT and FTIR spectroscopy of adsorbed CO.

Acknowledgements

S. Dzwigaj gratefully acknowledges CNRS (France) for financing his research position. Special thanks are due to C. Clodic (UPMC Univ Paris 6, UMR 7197, Laboratoire de Réactivité de Surface) for performed BET measurements.

References

[1] H. Ghobakar, O. Schaf, U. Guth, Prog. Solid State Chem. 27 (1999) 27.
[2] L.D. Li, Q. Shen, J.J. Yu, Z.P. Hao, Z.P. Xu, G.Q. Max Lu, Environ. Sci. Technol. 41 (2007) 7901.
[3] D.A. Bulushev, P.M. Prechtl, A. Renken, L. Kiwi-Minsker, Ind. Eng. Chem. Res. 46 (2000) 4178.
[4] L. Capek, J. Dedecek, B. Wichterlova, J. Catal. 227 (2004) 352.
[5] L. Gutierrez, M.A. Ulla, E.A. Lombardo, A. Kovacs, F. Lonyi, J. Valyon, Appl. Catal. 292 (2005) 154.
[6] A. Szegedi, M. Hegedus, J.L. Margitfalvi, I. Kiricsi, Chem. Commun. (2005) 1441.
[7] J.N. Lin, J.H. Chen, C.Y. Hsiao, Y.M. Kang, B.Z. Wan, Appl. Catal. B 36 (2002) 19.
[8] S. Dzwigaj, J. Janas, T. Machej, M. Che, Catal. Today 119 (2007) 133.
[9] J. Janas, J. Gurgul, R.P. Socha, T. Shishido, M. Che, S. Dzwigaj, Appl. Catal. B 91 (2009) 113.
[10] S. Dzwigaj, M.J. Peltre, P. Massiani, A. Davidson, M. Che, T. Sen, S. Sivasanker, Chem. Commun. (1998) 87.
[11] S. Dzwigaj, P. Massiani, A. Davidson, M. Che, J. Mol. Catal. 155 (2000) 169.
[12] J. Kanervo, Industrial Chemistry Publication Series, 2003, Espo, No. 16.
[13] I. Kocemba, Przemysł Chemiczny 82 (2003) 142.
[14] K. Hadjiivanov, E. Ivanova, R. Kefirov, J. Janas, A. Plesniar, S. Dzwigaj, M. Che, Micropor. Mesopor. Mater. 131 (2010) 1.
[15] N. Bogdanchikova, A. Simakov, E. Smoletseva, A. Pestryakov, H.M. Farias, J.A. Diaz, A. Tompos, M. Avalos, Appl. Surf. Sci. 254 (2008) 4075.
[16] B. Coq, M. Mauvezin, G. Delahay, S. Kieger, J. Catal. 195 (2000) 298.
[17] T.V. Voskoboinikov, H.Y. Chen, W.M.H. Schalter, Appl. Catal. B 19 (1998) 279.
[18] N.R.C.F. Machado, V. Calsavara, N.G.C. Astrath, C.K. Matsuda, A.P. Junior, M.L. Baesso, Fuel 84 (2005) 2064.
[19] S. Dzwigaj, L. Stievano, F.E. Wagner, M. Che, J. Phys. Chem. Solids 68 (2007) 1885.
[20] P. Wu, T. Komatsu, T. Yashima, Micropor. Mesopor. Mater. 20 (1998) 139.
[21] L. Capek, V. Kreibich, J. Dedecek, T. Grygar, B. Wichterlova, Z. Sobalik, J.A. Martens, R. Brosius, V. Tokarova, Micropor. Mesopor. Mater. 80 (2005) 279.
[22] M. Santhosh Kumar, M. Schwidder, W. Grunert, U. Bentrup, A. Bruckner, J. Catal. 239 (2006) 173.
[23] L.P. Oleksenko, I.V. Kuz'mich, V.K. Yatsimirskii, V.Ya. Zub, Theor. Exp. Chem. 36 (2000) 5.
[24] S.T. Hong, M. Matsuoka, M. Anpo, Catal. Lett. 107 (2006) 3.
[25] Y.M. Kang, B.Z. Wan, Catal. Today 35 (1997) 379.